IEEE Access
Multidisciplinary | Rapid Review | Open Access Journal

Received May 6, 2017, accepted June 7, 2017, date of publication July 25, 2017, date of current version August 14, 2017.

Digital Object Identifier 10.1109/ACCESS.2017.2719628

Low-Complexity Detection of High-Order QAM Faster-Than-Nyquist Signaling

EBRAHIM BEDEER[1], (Member, IEEE), MOHAMED HOSSAM AHMED[2], (Senior Member, IEEE), AND HALIM YANIKOMEROGLU[1], (Fellow, IEEE)
[1]System and Computer Engineering Department, Carleton University, Ottawa, ON K1S 5B6, Canada
[2]Faculty of Engineering and Applied Science, Memorial University of Newfoundland, St. John's, NL A1B 3X5, Canada

Corresponding author: Ebrahim Bedeer (e.bedeer@sce.carleton.ca)

This work was supported in part by DragonWave Inc., in part by the Mathematics of Information Technology and Complex Systems Canada, and in part by the Natural Science and Engineering Research Council of Canada through Discovery Program.

ABSTRACT Faster-than-Nyquist (FTN) signaling is a promising non-orthogonal transmission technique to considerably improve the spectral efficiency. This paper presents the first attempt in the literature to estimate the transmit data symbols of any high-order quadrature amplitude modulation (QAM) FTN signaling in polynomial time complexity. In particular, we propose a generalized approach to model the finite alphabet of any high-order QAM constellation as a high degree polynomial constraint. Then, we formulate the high-order QAM FTN signaling sequence estimation problem as a non-convex optimization problem. As an example of a high-order QAM, we consider 16-QAM FTN signaling and then transform the high degree polynomial constraint, with the help of auxiliary variables, to multiple quadratic constraints. Such transformation allows us to propose a generalized approach semidefinite relaxation (SDR)-based sequence estimation (GASDRSE) technique to efficiently provide a sub-optimal solution to the NP-hard non-convex FTN detection problem, with polynomial time complexity. For the particular case of 16-QAM FTN signaling, we additionally propose a sequence estimation technique based on concepts from the set theory. We show that the set theory SDR-based sequence estimation (STSDRSE) technique is of lower complexity when compared with the proposed GASDRSE. Simulation results show the effectiveness of the proposed GASDRSE and STSDRSE techniques in increasing the data rate and spectral efficiency of 16-QAM FTN signaling, without increasing the bit-error-rate, the bandwidth, or the data symbols energy, when compared with the Nyquist signaling.

INDEX TERMS Faster-than-Nyquist (FTN), high-order QAM, intersymbol interference (ISI), Mazo limit, semidefinite relaxation (SDR), sequence estimation.

I. INTRODUCTION

Higher spectrally efficient transmission techniques, e.g., faster-than-Nyquist (FTN) signaling, have attracted the attention of industrial and academic communities to meet the ever increasing demands on data rates [1]. In FTN signaling, the T-orthogonal pulses are sent at rate $\frac{1}{\tau T}$ which is higher than the Nyquist signaling rate $\frac{1}{T}$, where $0 < \tau \leq 1$ is the time packing parameter. Since FTN signaling violates the Nyquist limit, inter-symbol interference (ISI) between the received pulses is unavoidable.

The pioneering work of Mazo in [2] showed that FTN signaling does not affect the minimum distance of uncoded binary sinc pulse transmission, and hence the asymptotic error probability, as long as the time packing parameter τ is above a certain limit, i.e., $\tau \geq 0.802$, later known as Mazo limit. Mazo limit has been extended to root-raised cosine (rRC) pulses in [3], to frequency and time domains simultaneously in [4], and to multiple-input-multiple-output systems in [5].

Most of the research literature focused on the detection of binary or low-order quadrature amplitude modulation (QAM) FTN signaling [6]–[10]; this is mainly due to the excessive computational complexity involved in removing the ISI of high-order constellations FTN signaling. For instance, Bedeer *et al.* [6] proposed a reduced complexity sphere decoding algorithm to optimally detect binary FTN signaling. The reduction in complexity was achieved on average and not in the worst case sense. However, extending such an algorithm to high-order QAM results in prohibitive computational complexity. Similarly, extending the truncated state Viterbi algorithm (VA) [7] and the reduced state Bahl-Cocke-Jelinek-Raviv (BCJR) algorithm [8] to high-order QAM are not straightforward and rather lead to significant computational complexity. The worst case computational complexities of the works in [6]–[9] are in general exponential either in received block length [6] or the ISI length [7]–[9]. Bedeer *et al.* [10] proposed reduced complexity algorithms to detect binary and 4-QAM FTN signaling on symbol-by-symbol basis. Extending these algorithms to detect high-order QAM is not trivial and most likely will lead to unsatisfactory performance. In [11], a modified BCJR algorithm was proposed to detect 4-pulse amplitude modulation FTN signaling. In [12], a 9-QAM super-Nyquist signaling scheme is proposed for optical fiber communications to improve the spectral efficiency.

This paper presents the first attempt in the literature to detect FTN signaling of *any* high-order QAM constellation (and in particular 16-QAM constellation) in polynomial time complexity. More specifically, we propose a generalized approach to model the finite alphabet of any high-order QAM constellation as a high degree polynomial constraint, and we formulate the FTN signaling detection problem as a non-convex optimization problem that turns out to be non-deterministic polynomial-time (NP)-hard. This means the FTN detection problem is at least as hard as the hardest problems in NP [13]. As an example of a high-order QAM, we consider 16-QAM FTN signaling and use auxiliary variables to transform the high degree polynomial constraint to multiple quadratic constraint. That said, we propose a generalized approach semidefinite relaxation (SDR)-based sequence estimation (GASDRSE) technique to efficiently provide a sub-optimal solution to the NP-hard non-convex FTN signaling detection problem, with polynomial time complexity. For the particular case of 16-QAM FTN signaling, we additionally propose a sequence estimation technique based on concepts from the set theory. We show that the set theory SDR-based sequence estimation (STSDRSE) technique is of lower complexity when compared to the proposed GASDRSE. Simulation results show the effectiveness of the proposed GASDRSE and STSDRSE techniques, for moderate values of τ, in significantly increasing the data rate and spectrum efficiency of 16-QAM FTN signaling without increasing the BER, the bandwidth, or the data symbols energy, when compared to Nyquist signaling.

The remainder of this paper is organized as follows. Section II presents the system model of the high-order QAM FTN signaling and formulates the maximum likelihood sequence estimation (MLSE) detection problems. The proposed GASDRSE technique for the case of 16-QAM FTN signaling is discussed in Section III; while in Section IV we introduce the proposed STSDRSE technique. The computational complexities of the proposed algorithms are discussed in Section V. Section VI provides the simulation results, and finally the paper is concluded in Section VII.

Throughout the paper we use bold-faced upper case letters, e.g., $\boldsymbol{X}$, to denote matrices, bold-faced lower case letters, e.g., $\boldsymbol{x}$, to denote column vectors, and light-faced italics letters, e.g., x, to denote scalars. The complex conjugate of a complex number x is denoted as x^*, x_i denotes the ith element of vector $\boldsymbol{x}$ and $\text{tr}(\boldsymbol{X})$, $\text{rank}(\boldsymbol{X})$, and $\text{diag}(\boldsymbol{X})$ denote the trace, rank, and a column vector consisting of the diagonal elements of matrix $\boldsymbol{X}$, respectively. The operator $\mathbb{E}(.)$ denotes the expectation, $[.]^{\text{T}}$ denotes the transpose operator, $\boldsymbol{I}$ is the identity matrix, $\|.\|_p$ is the p-norm, and $\mathcal{N}(.,.)$ represents the Gaussian distribution. $\mathbf{1}$ denotes the vector of ones, $\Re\{.\}$ and $\Im\{.\}$ represent the real and imaginary parts of complex numbers, respectively.

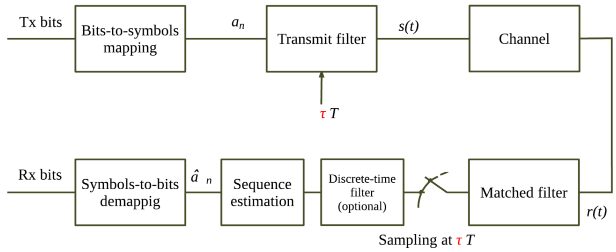

FIGURE 1. Block diagram of FTN signaling.

II. SYSTEM MODEL AND FTN SIGNALING DETECTION PROBLEM FORMULATION

Fig. 1 shows a block diagram of a communication system employing FTN signaling. Data bits to be transmitted are gray mapped[1] to data symbols through the bits-to-symbols mapping block. Data symbols are transmitted, through the transmit filter block, faster than the traditional Nyquist transmission, i.e., every τT, where $0 < \tau \leq 1$ is the time packing/acceleration parameter and T is the symbol duration. A possible receiver structure is shown in Fig. 1, where the received signal is passed through a filter matched to the transmit filter followed by a sampler and an optional discrete-time filter. Since the transmission rate of the transmit pulses carrying the data symbols intentionally violate the Nyquist criterion, ISI occurs between the received samples. Accordingly, sequence estimation techniques are needed to remove the ISI and to estimate the transmitted data symbols. The estimated data symbols are finally gray demapped to the estimated received bits.

The received FTN signal in case of additive white Gaussian noise (AWGN) channel is written as

$$\bar{y}(t) = \sqrt{\tau E_s} \sum_{n=1}^{N} \bar{a}_n g(t - n\tau T) + \bar{q}(t), \tag{1}$$

where N is the total number of transmit data symbols, $\bar{a}_n$, $n = 1, \ldots, N$, is the independent and identically distributed data symbols drawn from any high-order QAM constellation, E_s is the data symbol energy, $g(t) = \int p(x)p(x-t)dx$, where $p(t)$ is a real-valued and unit-energy pulse, i.e., $\int_{-\infty}^{\infty} |p(t)|^2 dt = 1$, $\bar{q}(t) = \int n(x)p(x - t)dx$ with $n(t)$ is the additive white Gaussian noise (AWGN) with zero mean and variance σ^2, and $1/(\tau T)$ is the signaling rate.

[1] In this paper, we focus on 16-QAM, and hence, gray mapping is possible. Optimization of the bits-to-symbol mapping is an interesting topic itself which is beyond the scope of this paper.

Assuming perfect time synchronization between the transmitter and the receiver, the received high-order QAM FTN signal $\bar{y}(t)$ is sampled every τT and the kth received sample is expressed as

$$\begin{aligned}\bar{y}_k &= \bar{y}(k\tau T),\\ &= \sqrt{\tau E_s}\sum_{n=1}^{N}\bar{a}_n g(k\tau T - n\tau T) + \bar{q}(k\tau T),\\ &= \underbrace{\sqrt{\tau E_s}\bar{a}_k g(0)}_{\text{desired symbol}} + \underbrace{\sqrt{\tau E_s}\sum_{n=1,n\neq k}^{N}\bar{a}_n g((k-n)\tau T)}_{\text{ISI}}\\ &\quad + \bar{q}(k\tau T).\end{aligned} \tag{2}$$

As can be seen, the kth received data symbol depends on the kth transmit data symbol, as well as, ISI from adjacent symbols.

A. FORMULATION OF THE HIGH-ORDER QAM FTN SIGNALING DETECTION PROBLEM FOR GENERAL PULSE SHAPE

The received FTN signal after the matched filter and sampler can be written in a vector form as

$$\bar{\boldsymbol{y}}_{\rm c} = \bar{\boldsymbol{G}}\bar{\boldsymbol{a}} + \bar{\boldsymbol{q}}_{\rm c}, \tag{3}$$

where $\bar{\boldsymbol{y}}_{\rm c}$ is the $N \times 1$ received samples vector that contains colored noise samples, $\bar{\boldsymbol{G}}$ is the $N \times N$ intersymbol interference (ISI) matrix,[2] $\bar{\boldsymbol{a}}$ is the $N \times 1$ transmitted data symbols vector, and $\bar{\boldsymbol{q}}_{\rm c} \sim \mathcal{N}(0, \sigma^2\bar{\boldsymbol{G}})$ is the $N \times 1$ Gaussian noise samples with zero-mean and covariance matrix $\sigma^2\bar{\boldsymbol{G}}$ [6].

To avoid handling complex-valued variables, we use the following equivalent real-valued model of (3) as follows[3]

$$\begin{aligned}\boldsymbol{y}_{{\rm c},2N\times 1} &= \boldsymbol{G}_{2N\times 2N}\boldsymbol{a}_{2N\times 1} + \boldsymbol{q}_{{\rm c},2N\times 1},\\ \begin{bmatrix}\Re\{\bar{\boldsymbol{y}}_{\rm c}\}\\ \Im\{\bar{\boldsymbol{y}}_{\rm c}\}\end{bmatrix} &= \begin{bmatrix}\Re\{\bar{\boldsymbol{G}}\} & -\Im\{\bar{\boldsymbol{G}}\}\\ \Im\{\bar{\boldsymbol{G}}\} & \Re\{\bar{\boldsymbol{G}}\}\end{bmatrix}\begin{bmatrix}\Re\{\bar{\boldsymbol{a}}\}\\ \Im\{\bar{\boldsymbol{a}}\}\end{bmatrix} + \begin{bmatrix}\Re\{\bar{\boldsymbol{q}}_{\rm c}\}\\ \Im\{\bar{\boldsymbol{q}}_{\rm c}\}\end{bmatrix}.\end{aligned} \tag{4}$$

Assuming that $\boldsymbol{G}$ is invertible, one can rewrite (4) as

$$\begin{aligned}\boldsymbol{G}^{-1}\boldsymbol{y}_{\rm c} &= \boldsymbol{a} + \boldsymbol{G}^{-1}\boldsymbol{q}_{\rm c},\\ \boldsymbol{z} &= \boldsymbol{a} + \boldsymbol{\eta},\end{aligned} \tag{5}$$

where $\boldsymbol{z} = \boldsymbol{G}^{-1}\boldsymbol{y}_{\rm c}$ and $\boldsymbol{\eta} = \boldsymbol{G}^{-1}\boldsymbol{q}_{\rm c}$. The high-order QAM FTN signaling sequence estimation problem can be interpreted as follows. Given the received samples $\boldsymbol{z}$ (or $\boldsymbol{y}_{\rm c}$), we want to find an estimated data symbol vector $\hat{\boldsymbol{a}}$, to the transmit data symbol vector $\boldsymbol{a}$, such that the probability of error is minimized. In other words, the FTN detection problem can be seen as a maximization of the probability that the data symbol vector $\boldsymbol{a}$ is sent given the received samples $\boldsymbol{z}$ (or $\boldsymbol{y}_{\rm c}$). With the help of Bayes rule, such maximization problem can be re-expressed equivalently as

$$\hat{\boldsymbol{a}} = \arg\max_{\boldsymbol{a}\in\mathcal{D}} P\left(\boldsymbol{z}|\boldsymbol{a}\right). \tag{6}$$

[2]The ISI matrix matrix $\boldsymbol{G}$ is a Toeplitz matrix, and hence, some errors may occur at the boundaries between data blocks. Ideas of overlap and reject can be employed to mitigate such errors.

[3]One can use the structure in (4) (i.e., the fact that the real and imaginary parts of the received signal and noise are independent and the fact that the imaginary part of the ISI matrix is zero for the case of AWGN channel) to implement the proposed algorithms in parallel, i.e., by separately processing the real and imaginary parts of the received signal.

The probability $P\left(\boldsymbol{z}|\boldsymbol{a}\right)$ is usually known as the likelihood probability, and hence, the problem to estimate the received symbol vector $\hat{\boldsymbol{a}}$ is known as the maximum likelihood sequence estimation (MLSE) problem.

Following (5), for a given set of data symbols $\boldsymbol{a}$, the received samples $\boldsymbol{z}$ can be seen as Gaussian random variables with a mean $\boldsymbol{a}$ and covariance matrix $\frac{1}{2}\sigma^2\boldsymbol{G}^{-1}$, i.e., $\boldsymbol{\eta} \in \mathcal{N}(0, \frac{1}{2}\sigma^2\boldsymbol{G}^{-1})$ (the proof is provided in Appendix). That said, the likelihood probability in (6) to detect the high-order QAM FTN signaling is expressed as [14]

$$P(\boldsymbol{z}|\boldsymbol{a}) = \left(\frac{1}{2\pi\sigma^2}\right)^{N/2}\frac{1}{\sqrt{\det[\boldsymbol{G}^{-1}]}} \times \exp\left(-\frac{1}{\sigma^2}(\boldsymbol{z}-\boldsymbol{a})^{\rm T}\boldsymbol{G}(\boldsymbol{z}-\boldsymbol{a})\right). \tag{7}$$

One can see from (7) that maximizing the likelihood function is equivalent to maximizing the exponent of the exponential function (or minimize its negative value). Accordingly, the MLSE problem to detect high-order QAM FTN signaling is written as

$$\mathcal{OP}_{{\rm MLSE}_{\rm c}}: \hat{\boldsymbol{a}} = \arg\min_{\boldsymbol{a}\in\mathcal{D}}(\boldsymbol{z}-\boldsymbol{a})^{\rm T}\boldsymbol{G}(\boldsymbol{z}-\boldsymbol{a}). \tag{8}$$

B. FORMULATION OF THE HIGH-ORDER QAM FTN SIGNALING DETECTION PROBLEM FOR rRC PULSE SHAPE

Equation (5) assumes the ISI matrix $\boldsymbol{G}$ is invertible. However, this does not necessarily hold for common pulse shapes such as rRC pulses operating at very small values of τ [7]. In such cases, designing a causal and stable whitening matched filter is necessary, and we follow a designing approach similar to the one in [7]. That said, (2) can be re-written as

$$\bar{\boldsymbol{y}}_{\rm c} = \sqrt{\tau E_s}\bar{\boldsymbol{a}} \star \boldsymbol{g} + \bar{\boldsymbol{q}}_{\rm c}, \tag{9}$$

where $\star$ denotes the convolution operator. The whitening filter decorrelates the noise $\bar{\boldsymbol{q}}_{\rm c}$ and can be constructed from $\boldsymbol{g}$ by spectral factorization of its all-zero z-transform $G(z)$ into $V(z)V(1/z^*)$ [15]. After whitening the received vector $\bar{\boldsymbol{y}}_{\rm c}$ by $1/V(1/z^*)$, the whitened received vector can be represented as

$$\bar{\boldsymbol{y}}_{\rm w} = \sqrt{\tau E_s}\bar{\boldsymbol{a}} \star \boldsymbol{v} + \bar{\boldsymbol{q}}_{\rm w}, \tag{10}$$

where $\bar{\boldsymbol{q}}_{\rm w}$ is white Gaussian noise with zero mean and variance σ^2 and $\boldsymbol{v}$ represents the causal ISI such that $\boldsymbol{v}[n] \star \boldsymbol{v}[-n] = \boldsymbol{g}$. It is not possible to design an exact whitening filter, i.e. to have $V(z)$ with all zeros strictly outside the unit circle, especially for very small values of τ. That said, we design approximate whitening filter as follows [7]. We find $G(z)$ with quartets of zeros on the unit circle (zeros has to occur in quartets as $V(z)$ and $V(1/z^*)$ each requires a conjugate pair). Then, we split the quartet of zeros such that one conjugate pair is slightly inside the unit circle and one is outside. Our aim is to have the spectrum of approximation whitening filter $1/V(1/z^*)$ and channel model $V(z)$ as close as possible to the the spectrum of $\boldsymbol{g}$. Equation (10) can be written in a vector form as

$$\bar{\boldsymbol{y}}_{\mathrm{w}} = \overline{\boldsymbol{V}}\bar{\boldsymbol{a}} + \bar{\boldsymbol{q}}_{\mathrm{w}}, \tag{11}$$

where $\overline{\boldsymbol{V}}$ is the ISI matrix constructed from the vector $\boldsymbol{v}$. Similar to the previous discussion, we use the following equivalent real-valued model of (11) as follows

$$\begin{aligned} \boldsymbol{y}_{\mathrm{w},2N\times 1} &= \boldsymbol{V}_{2N\times 2N}\,\boldsymbol{a}_{2N\times 1} + \boldsymbol{q}_{\mathrm{w},2N\times 1}, \\ \begin{bmatrix} \Re\{\bar{\boldsymbol{y}}_{\mathrm{w}}\} \\ \Im\{\bar{\boldsymbol{y}}_{\mathrm{w}}\} \end{bmatrix} &= \begin{bmatrix} \Re\{\overline{\boldsymbol{V}}\} & -\Im\{\overline{\boldsymbol{V}}\} \\ \Im\{\overline{\boldsymbol{V}}\} & \Re\{\overline{\boldsymbol{V}}\} \end{bmatrix} \begin{bmatrix} \Re\{\bar{\boldsymbol{a}}\} \\ \Im\{\bar{\boldsymbol{a}}\} \end{bmatrix} + \begin{bmatrix} \Re\{\bar{\boldsymbol{q}}_{\mathrm{w}}\} \\ \Im\{\bar{\boldsymbol{q}}_{\mathrm{w}}\} \end{bmatrix}. \end{aligned} \tag{12}$$

Similar to the previous discussion, we can formulate the high-order QAM FTN signaling detection problem as

$$\mathcal{OP}_{\mathrm{MLSE_w}}: \quad \hat{\boldsymbol{a}} = \arg\min_{\boldsymbol{a}\in\mathcal{D}} \|\boldsymbol{y}_{\mathrm{w}} - \boldsymbol{V}\boldsymbol{a}\|_2^2. \tag{13}$$

C. COMMENTS ON COMPLEXITY OF OPTIMAL DETECTION OF HIGH-ORDER QAM FTN SIGNALING DETECTION PROBLEMS

The $\mathcal{OP}_{\mathrm{MLSE_c}}$ and $\mathcal{OP}_{\mathrm{MLSE_w}}$ problems can be solved by a brute force search with a complexity in the order of M^{2N}, where M is the modulation order of the transmit symbols of the real-valued model in (4) or (12). However, such extensive computational complexity hinders the MLSE practical implementations. Other techniques such as BCJR [8], [9], Viterbi algorithm [7], and sphere decoding [6] (that approximate the optimal detection of the $\mathcal{OP}_{\mathrm{MLSE_c}}$ and $\mathcal{OP}_{\mathrm{MLSE_w}}$ problems) require an exponential (in ISI length at best) worst case computational complexity. In the following sections, we propose reduced-complexity SDR-based sequence estimation techniques, namely, GASDRSE and STSDRSE techniques, to provide a suboptimal solution to the $\mathcal{OP}_{\mathrm{MLSE_c}}$ and $\mathcal{OP}_{\mathrm{MLSE,w}}$ problems, with polynomial time complexity.

III. PROPOSED GASDRSE TECHNIQUE

In this section, we propose a generalized approach reduced-complexity SDR-based sequence estimation technique that provides a sub-optimal solution for the detection of any high-QAM FTN signaling.

A. FORMULATION OF QUADRATIC CONSTRAINTS

In order to transform the $\mathcal{OP}_{\mathrm{MLSE_c}}$ and $\mathcal{OP}_{\mathrm{MLSE,w}}$ in (8) and (13), respectively, to an SDR problem, we make use of the following observation. Any finite alphabet constellation can be replaced by a high degree polynomial constraint [16], e.g., if $x \in \{x_1, x_2, \ldots, x_M\}$, then $(x - x_1)(x - x_2)\ldots(x-x_M) = 0$. Next, by introducing appropriate auxiliary variables, the high degree polynomial constraint can be replaced by multiple quadratic constraints.

In our case of interest, i.e., 16-QAM, the set $\mathcal{D}$ in $\mathcal{OP}_{\mathrm{MLSE_c}}$ and $\mathcal{OP}_{\mathrm{MLSE_w}}$ includes the constellation points whose real and imaginary parts belong to the set $\{\pm 1, \pm 3\}$, and hence, the high degree polynomial constraint can be written as

$$(a_n - 1)(a_n + 1)(a_n - 3)(a_n + 3) = 0, \quad n = 1, \ldots, 2N. \tag{14}$$

By introducing the auxiliary variables $b_n = a_n^2, n = 1, \ldots, 2N$, the constraints in (14) can be further written as

$$a_n^2 - b_n = 0, \quad n = 1, \ldots, 2N, \tag{15}$$

$$b_n^2 - 10b_n + 9 = 0, \quad n = 1, \ldots, 2N. \tag{16}$$

To facilitate formulating the SDR sequence estimation problem, we define the following $4N \times 1$ column vector

$$\boldsymbol{\omega}^{\mathrm{T}} = [\boldsymbol{a}^{\mathrm{T}}\boldsymbol{b}^{\mathrm{T}}1], \tag{17}$$

and we find the rank-one positive semidefinite matrix $\boldsymbol{\Omega} = \boldsymbol{\omega}\boldsymbol{\omega}^{\mathrm{T}}$ (of dimension $(4N+1) \times (4N+1)$) as

$$\boldsymbol{\Omega} = \begin{bmatrix} \boldsymbol{a}\boldsymbol{a}^{\mathrm{T}} & \boldsymbol{a}\boldsymbol{b}^{\mathrm{T}} & \boldsymbol{a} \\ \boldsymbol{b}\boldsymbol{a}^{\mathrm{T}} & \boldsymbol{b}\boldsymbol{b}^{\mathrm{T}} & \boldsymbol{b} \\ \boldsymbol{a}^{\mathrm{T}} & \boldsymbol{b}^{\mathrm{T}} & 1 \end{bmatrix}. \tag{18}$$

The constraints in (15) and (16) can be re-expressed in terms of $\boldsymbol{\Omega}$, as

$$\mathrm{diag}\{\boldsymbol{\Omega}_{1,1}\} - \boldsymbol{\Omega}_{2,3} = 0, \tag{19}$$

$$\mathrm{diag}\{\boldsymbol{\Omega}_{2,2}\} - 10\boldsymbol{\Omega}_{2,3} + 9.\boldsymbol{1} = 0, \tag{20}$$

$$\boldsymbol{\Omega}_{3,3} = 1, \tag{21}$$

where $\boldsymbol{\Omega}_{i,j}$, $i, j = 1, 2$, and 3, are the (i, j)th sub-blocks of $\boldsymbol{\Omega}$ of appropriate sizes, e.g., $\boldsymbol{\Omega}_{1,1} = \boldsymbol{a}\boldsymbol{a}^{\mathrm{T}}$ (of size $2N \times 2N$), $\boldsymbol{\Omega}_{2,3} = \boldsymbol{b}$ (of size $2N \times 1$), $\boldsymbol{\Omega}_{2,2} = \boldsymbol{b}\boldsymbol{b}^{\mathrm{T}}$ (of size $2N \times 2N$), $\boldsymbol{\Omega}_{1,3} = \boldsymbol{a}$, and $\boldsymbol{\Omega}_{3,3} = 1$.

B. FORMULATION OF OBJECTIVE FUNCTION

1) GENERAL PULSE SHAPE

Since the matrix $\boldsymbol{G}$ is symmetric, the objective function of $\mathcal{OP}_{\mathrm{MLSE_c}}$ in (8) can be rewritten in terms of $\boldsymbol{\Omega}$ as [16], [17]

$$\boldsymbol{\omega}^{\mathrm{T}}\boldsymbol{\Phi}_{\mathrm{c}}\boldsymbol{\omega} = \mathrm{tr}\{\boldsymbol{\Phi}_{\mathrm{c}}\boldsymbol{\omega}\boldsymbol{\omega}^{\mathrm{T}}\} = \mathrm{tr}\{\boldsymbol{\Phi}_{\mathrm{c}}\boldsymbol{\Omega}\}, \tag{22}$$

where

$$\boldsymbol{\Phi}_{c,(4N+1)\times(4N+1)} = \begin{bmatrix} \boldsymbol{G} & \boldsymbol{0} & -\boldsymbol{y}_{\mathrm{c}} \\ \boldsymbol{0} & \boldsymbol{0} & \boldsymbol{0} \\ -\boldsymbol{y}_{\mathrm{c}}^{\mathrm{T}} & \boldsymbol{0} & \boldsymbol{z}^{\mathrm{T}}\boldsymbol{G}\boldsymbol{z} \end{bmatrix}. \tag{23}$$

2) rRC PULSE SHAPE

For the case of rRC and given that the matrix $\boldsymbol{V}$ is symmetric, the objective function of $\mathcal{OP}_{\mathrm{MLSE_w}}$ in (13) can be rewritten in terms of $\boldsymbol{\Omega}$ as [16], [17]

$$\mathrm{tr}\{\boldsymbol{\Phi}_{\mathrm{w}}\boldsymbol{\Omega}\}, \tag{24}$$

where $\boldsymbol{\Phi}_{\mathrm{w}}$ is given by

$$\boldsymbol{\Phi}_{\mathrm{w},(4N+1)\times(4N+1)} = \begin{bmatrix} \boldsymbol{V}^{\mathrm{T}}\boldsymbol{V} & \boldsymbol{0} & -\boldsymbol{V}^{\mathrm{T}}\boldsymbol{y}_{\mathrm{w}} \\ \boldsymbol{0} & \boldsymbol{0} & \boldsymbol{0} \\ -\boldsymbol{y}_{\mathrm{w}}^{\mathrm{T}}\boldsymbol{V} & \boldsymbol{0} & \boldsymbol{y}_{\mathrm{w}}^{\mathrm{T}}\boldsymbol{y}_{\mathrm{w}} \end{bmatrix}. \tag{25}$$

C. SDR OPTIMIZATION PROBLEM AND PROPOSED GASDRSE ALGORITHM

Finally, the optimization problems $\mathcal{OP}_{\text{MLSE}_\text{c}}$ and $\mathcal{OP}_{\text{MLSE}_\text{w}}$ in (8) and (13), respectively, to detect 16-QAM FTN signaling is re-expressed as

$$\begin{aligned}&\min_{\boldsymbol{\Omega}} \ \text{tr}\{\boldsymbol{\Phi}\boldsymbol{\Omega}\}\\ &\text{subject to (19), (20), and (21),}\\ &\qquad\qquad \boldsymbol{\Omega} \succeq 0, && (26)\\ &\qquad\qquad \text{rank}\{\boldsymbol{\Omega}\} = 1, && (27)\end{aligned}$$

where $\boldsymbol{\Phi} \in \{\boldsymbol{\Phi}_\text{c}, \boldsymbol{\Phi}_\text{w}\}$ and the constraints in (26) and (27) are used to reflect that $\boldsymbol{\Omega}$ is a positive semidefinite and a rank-one matrix, respectively. Such an optimization problem is non-convex due to the rank-one constraint in (27). By relaxing this constraint, we obtain an upper bound on its optimal solution as

$$\mathcal{OP}_{\text{GASDRSE}}: \quad \min_{\boldsymbol{\Omega}} \ \text{tr}\{\boldsymbol{\Phi}\boldsymbol{\Omega}\} \quad \text{subject to (19), (20), (21), and (26).}$$

Please note that the objective function of $\mathcal{OP}_{\text{GASDRSE}}$ is linear in $\boldsymbol{\Omega}$ subject to affine equalities and a linear matrix inequality.

The optimization problem $\mathcal{OP}_{\text{GASDRSE}}$ can be efficiently solved to any arbitrary accuracy using well-developed reliable numerical solvers [18]. By solving $\mathcal{OP}_{\text{GASDRSE}}$, we obtain the optimal solution $\boldsymbol{\Omega}_\text{op}$ which is the global optimal solution to the convex problem $\mathcal{OP}_{\text{GASDRSE}}$. In order to obtain a feasible solution to the original non-convex FTN detection problem, we use Gaussian randomization [17]. The intuition behind Gaussian randomization is to solve a stochastic version of $\mathcal{OP}_{\text{GASDRSE}}$, where the sub-optimal solution $\hat{\boldsymbol{w}}$ is considered as the random vector—generated from a multivariate Gaussian random vector with zero mean and covariance matrix $\boldsymbol{\Omega}_\text{op}$—that maximizes the objective in $\mathcal{OP}_{\text{GASDRSE}}$. The Gaussian randomization procedure can be explained as follows. We generate $\boldsymbol{\xi}_\ell, \ell = 1, \ldots, L$, where L is the total number of randomization iterations, as $\boldsymbol{\xi}_\ell \sim (\mathbf{0}, \boldsymbol{\Omega}_\text{op})$, then we find $\breve{\boldsymbol{\omega}}_\ell = \text{quantize}\{\boldsymbol{\xi}_\ell\}$, where quantize$(x)$ rounds x to the nearest element in the set $\{\pm1, \pm3\}$. Then, we select the optimal value of ℓ, i.e., ℓ_op, that minimizes the objective function in $\mathcal{OP}_{\text{GASDRSE}}$ as

$$\ell_\text{op} = \arg \min_{\ell=1,\ldots,L} \text{tr}\{\boldsymbol{\Phi}\breve{\boldsymbol{\omega}}_\ell\breve{\boldsymbol{\omega}}_\ell^\text{T}\}, \tag{28}$$

where one can easily find the sub-optimal vector $\hat{\boldsymbol{\omega}}$ as

$$\hat{\boldsymbol{\omega}} = \breve{\boldsymbol{\omega}}_{\ell_\text{op}}. \tag{29}$$

Finally, the estimated data symbols vector $\hat{\boldsymbol{a}}$ can be found from the first $2N$ elements in $\hat{\boldsymbol{\omega}}$.

The proposed GASDRSE technique is formally expressed in Algorithm 1 as follows

Algorithm 1: Proposed GASDRSE Technique

1) **Input:** Pulse shape $p(t)$ (ISI matrix $\boldsymbol{G}$), received samples $\boldsymbol{y}_\text{c}$ or $\boldsymbol{y}_\text{w}$, and number of randomization iterations L.
2) Solve $\mathcal{OP}_{\text{GASDRSE}}$ to find $\boldsymbol{\Omega}_\text{op}$.
3) Generate random variable $\boldsymbol{\xi}_\ell$ as $\boldsymbol{\xi}_\ell \sim (0, \boldsymbol{\Omega}_\text{op})$, $\ell = 1, \ldots, L$.
4) Find $\breve{\boldsymbol{\omega}}_\ell = \text{quantize}\{\boldsymbol{\xi}_\ell\}$.
5) Find $\ell_\text{op} = \arg \min_{\ell=1,\ldots,L} \text{tr}\{\boldsymbol{\Phi}\breve{\boldsymbol{\omega}}_\ell\breve{\boldsymbol{\omega}}_\ell^\text{T}\}$.
6) Set $\hat{\boldsymbol{\omega}} = \breve{\boldsymbol{\omega}}_{\ell_\text{op}}$.
7) **Output:** The estimated data symbols $\hat{\boldsymbol{a}}$ which are the first $2N$ elements of $\hat{\boldsymbol{\omega}}$.

IV. PROPOSED STSDRSE TECHNIQUE

In this section, we propose a STSDRSE technique to detect 16-QAM FTN signaling with reduced complexity. The proposed sequence estimation technique is more computationally efficient when compared to the proposed GASDRSE. As can be seen in $\mathcal{OP}_{\text{GASDRSE}}$, the dimension of the decision matrix $\boldsymbol{\Omega}$ is $(4N + 1) \times (4N + 1)$, where N is the length of the complex data symbol vector. In this section, we reduce the dimension of the decision matrix, and hence, decrease the computational complexity.

A. FORMULATION OF QUADRATIC CONSTRAINTS

We replace the generic high degree polynomial constraint that models any high-order QAM, using concepts from the set theory, with a set of quadratic constraints suited to our particular case of interest in this paper, i.e., 16-QAM. Towards this goal, let us define the following sets

$$\begin{aligned}\mathcal{D}_1 &:= (-\infty, -3),\\ \mathcal{D}_2 &:= (-3, -1),\\ \mathcal{D}_3 &:= (-1, 1),\\ \mathcal{D}_4 &:= (1, 3),\\ \mathcal{D}_5 &:= (3, \infty).\end{aligned} \tag{30}$$

Then, the constraints in $\mathcal{OP}_{\text{MLSE}_\text{c}}$ and $\mathcal{OP}_{\text{MLSE}_\text{w}}$ can be expressed as [16]

$$\{\pm1, \pm3\} = \overline{\mathcal{D}_1 \cup \mathcal{D}_2 \cup \mathcal{D}_3 \cup \mathcal{D}_4 \cup \mathcal{D}_5}. \tag{31}$$

With the help of De Morgan's associative laws [19], the constraints can be further rewritten as

$$\begin{aligned}\{\pm1, \pm3\} &= \overline{\mathcal{D}_1} \cap \overline{\mathcal{D}_2} \cap \overline{\mathcal{D}_3} \cap \overline{\mathcal{D}_4} \cap \overline{\mathcal{D}_5},\\ &= ((\overline{\mathcal{D}_1} \cap \overline{\mathcal{D}_5}) \cap \overline{\mathcal{D}_3}) \cap \overline{\mathcal{D}_2} \cap \overline{\mathcal{D}_4}\\ &= ([-3, -1] \cup [1, 3]) \cap \overline{\mathcal{D}_2} \cap \overline{\mathcal{D}_4}.\end{aligned} \tag{32}$$

Accordingly, $[-3, -1] \cup [1, 3]$, $\overline{\mathcal{D}_2}$, and $\overline{\mathcal{D}_2}$ can be respectively written as

$$1 \le a_n^2 \le 9, \tag{33}$$

$$(a_n + 1)(a_n + 3) \ge 0, \tag{34}$$

$$(a_n - 1)(a_n - 3) \ge 0. \tag{35}$$

To facilitate formulating the new SDR problem, let us reformulate $\mathcal{OP}_{\text{MLSE}_\text{c}}$ and $\mathcal{OP}_{\text{MLSE}_\text{w}}$ in a higher dimension by defining

$$\boldsymbol{\psi}^{\text{T}} = [\boldsymbol{a}^{\text{T}} 1],$$
$$\boldsymbol{\Psi}_{(2N+1)\times(2N+1)} = \boldsymbol{\psi}\boldsymbol{\psi}^{\text{T}} = \begin{bmatrix} \boldsymbol{a}\boldsymbol{a}^{\text{T}} & \boldsymbol{a} \\ \boldsymbol{a}^{\text{T}} & 1 \end{bmatrix}. \quad (36)$$

The constraints in (33) - (35) can be re-written in terms of $\boldsymbol{\Psi}$ as

$$\mathbf{1} \preceq \text{diag}\{\boldsymbol{\Psi}_{1,1}\} \preceq 9.\mathbf{1}, \quad (37)$$
$$\text{diag}\{\boldsymbol{\Psi}_{1,1}\} + 4\boldsymbol{\Psi}_{1,2} + 3.\mathbf{1} \succeq 0, \quad (38)$$
$$\text{diag}\{\boldsymbol{\Psi}_{1,1}\} - 4\boldsymbol{\Psi}_{1,2} + 3.\mathbf{1} \succeq 0, \quad (39)$$
$$\boldsymbol{\Psi}_{2,2} = 1, \quad (40)$$

where $\boldsymbol{\Psi}_{i,j}$, $i, j = 1, 2$ are the (i, j)th sub-blocks of $\boldsymbol{\Psi}$ of appropriate sizes, e.g., $\boldsymbol{\Psi}_{1,1} = \boldsymbol{a}\boldsymbol{a}^{\text{T}}$ (of size $2N \times 2N$), $\boldsymbol{\Psi}_{1,2} = \boldsymbol{a}$, $\boldsymbol{\Psi}_{2,1} = \boldsymbol{a}^{\text{T}}$, and $\boldsymbol{\Psi}_{2,2} = 1$. The constraints in (37), (38), and (39) are equivalent to (33), (34), and (35), respectively.

B. FORMULATION OF OBJECTIVE FUNCTION

1) GENERAL PULSE SHAPE

Since the matrix $\boldsymbol{G}$ is symmetric, the objective function of $\mathcal{OP}_{\text{MLSE}_\text{c}}$ can be expressed in terms of $\boldsymbol{\Psi}$ as [16], [17]

$$\boldsymbol{\psi}^{\text{T}}\boldsymbol{\Theta}_{\text{c}}\boldsymbol{\psi} = \text{tr}\{\boldsymbol{\Theta}_{\text{c}}\boldsymbol{\psi}\boldsymbol{\psi}^{\text{T}}\} = \text{tr}\{\boldsymbol{\Theta}_{\text{c}}\boldsymbol{\Psi}\}, \quad (41)$$

where

$$\boldsymbol{\Theta}_{\text{c},(2N+1)\times(2N+1)} = \begin{bmatrix} \boldsymbol{G} & -\boldsymbol{y}_{\text{c}} \\ -\boldsymbol{y}_{\text{c}}^{\text{T}} & \boldsymbol{z}^{\text{T}}\boldsymbol{G}\boldsymbol{z} \end{bmatrix}. \quad (42)$$

2) rRC PULSE SHAPE

For the case of rRC and for symmetric ISI matrix $\boldsymbol{V}$, the objective function of $\mathcal{OP}_{\text{MLSE}_\text{w}}$ in (13) can be rewritten in terms of $\boldsymbol{\Psi}$ as [16], [17]

$$\text{tr}\{\boldsymbol{\Theta}_{\text{w}}\boldsymbol{\Psi}\}, \quad (43)$$

where $\boldsymbol{\Theta}_{\text{w}}$ is given by

$$\boldsymbol{\Theta}_{\text{w}} = \begin{bmatrix} \boldsymbol{V}^{\text{T}}\boldsymbol{V} & -\boldsymbol{V}^{\text{T}}\boldsymbol{y}_{\text{w}} \\ -\boldsymbol{y}_{\text{w}}^{\text{T}}\boldsymbol{V} & \boldsymbol{y}_{\text{w}}^{\text{T}}\boldsymbol{y}_{\text{w}} \end{bmatrix}. \quad (44)$$

C. SDR OPTIMIZATION PROBLEM AND PROPOSED STSDRSE ALGORITHM

Finally, $\mathcal{OP}_{\text{MLSE}_\text{c}}$ and $\mathcal{OP}_{\text{MLSE}_\text{w}}$ can be casted as the following optimization problem

$$\min_{\boldsymbol{\Psi}} \ \text{tr}\{\boldsymbol{\Theta}\boldsymbol{\Psi}\}$$
subject to (37), (38), (39), and (40)
$$\boldsymbol{\Psi} \succeq 0, \quad (45)$$
$$\text{rank}\{\boldsymbol{\Psi}\} = 1, \quad (46)$$

where $\boldsymbol{\Theta} \in \{\boldsymbol{\Theta}_{\text{c}}, \boldsymbol{\Theta}_{\text{w}}\}$ and the constraints (45) and (46) reflect that $\boldsymbol{\Psi}$ is a positive semidefinite and a rank-one matrix, respectively. It is clear that the above optimization problem is not convex due to the rank-one constraint in (46). By relaxing this constraint, we obtain an upper bound on its optimal solution as

$$\mathcal{OP}_{\text{STSDRSE}}: \quad \min_{\boldsymbol{\Psi}} \ \text{tr}\{\boldsymbol{\Theta}\boldsymbol{\Psi}\}$$
subject to (37), (38), (39), (40), and (45),

which can be solved efficiently [18] with polynomial time complexity.

Similar to the previous discussion of the proposed GASDRSE, the optimal solution $\boldsymbol{\Psi}_{\text{op}}$ of $\mathcal{OP}_{\text{STSDRSE}}$ will not necessarily be a feasible solution of the original non-convex optimization problem; hence, we use Gaussian randomization to obtain an efficient feasible solution. We generate $\boldsymbol{\zeta}_\ell$, $\ell = 1, \ldots, L$, as $\boldsymbol{\zeta}_\ell \sim (\mathbf{0}, \boldsymbol{\Psi}_{\text{op}})$, then we quantized each random variable as $\breve{\boldsymbol{\psi}}_\ell = \text{quantize}\{\boldsymbol{\zeta}_\ell\}$. Finally, we find the solution as

$$\ell_{\text{op}} = \arg \min_{\ell=1,\ldots,L} \text{tr}\{\boldsymbol{\Theta}\breve{\boldsymbol{\psi}}_\ell\breve{\boldsymbol{\psi}}_\ell^{\text{T}}\}, \quad (47)$$
$$\hat{\boldsymbol{\psi}} = \breve{\boldsymbol{\psi}}_{\ell_{\text{op}}}. \quad (48)$$

Finally, the estimated 16-QAM constellation vector $\hat{\boldsymbol{a}}$ is found from the first $2N$ elements in the vector $\hat{\boldsymbol{\psi}}$.

The proposed STSDRSE technique is formally expressed in Algorithm 2 as follows

Algorithm 2: Proposed STSDRSE Technique

1) **Input:** Pulse shape $g(t)$ (ISI matrix $\boldsymbol{G}$), received samples $\boldsymbol{y}_{\text{c}}$ and $\boldsymbol{y}_{\text{w}}$, and number of randomization iterations L.
2) Solve $\mathcal{OP}_{\text{STSDRSE}}$ to find $\boldsymbol{\Psi}_{\text{op}}$.
3) Generate random variable $\boldsymbol{\zeta}_\ell$ as $\boldsymbol{\zeta}_\ell \sim (0, \boldsymbol{\Psi}_{\text{op}})$, $\ell = 1, \ldots, L$.
4) Find $\breve{\boldsymbol{\psi}}_\ell = \text{quantize}\{\boldsymbol{\zeta}_\ell\}$.
5) Find $\ell_{\text{op}} = \arg \min_{\ell=1,\ldots,L} \text{tr}\{\boldsymbol{\Theta}\breve{\boldsymbol{\psi}}_\ell\breve{\boldsymbol{\psi}}_\ell^{\text{T}}\}$.
6) Set $\hat{\boldsymbol{\psi}} = \breve{\boldsymbol{\psi}}_{\ell_{\text{op}}}$.
7) **Output:** Estimated data symbols $\hat{\boldsymbol{a}}$ are the first $2N$ elements of $\hat{\boldsymbol{\psi}}$.

V. COMMENTS ON THE PROPOSED GASDRSE AND STSDRSE TECHNIQUES

A. COMPLEXITY DISCUSSION

The worst case computational complexity of solving the relaxed $\mathcal{OP}_{\text{GASDRSE}}$ is $\mathcal{O}((4N + 1)^{3.5}$ [17]. Additionally, the complexity of generating and evaluating the objective function corresponding to the L random samples of the Gaussian randomization is $\mathcal{O}((4N + 1)^2 L$ [17]. Hence, the total computational complexity of the proposed GASDRSE technique is $\mathcal{O}((4N + 1)^{3.5} + (4N + 1)^2 L)$, which is polynomial in the received block length.

As mentioned earlier, the proposed GASDRSE technique can be extended to any high-order QAM FTN signaling, with polynomial time computational complexity. For instance, for the case of 64-QAM FTN signaling, we need to use an additional auxiliary variable $c_n = b_n^2, n = 1, \dots, 2N$, in order to formulate the detection problem. In this case, the complexity of solving the relaxed $\mathcal{OP}_{\text{GASDRSE}}$ is $\mathcal{O}((6N+1)^{3.5}$, and the complexity of generating and evaluating the objective function corresponding to the L random samples of the Gaussian randomization is $\mathcal{O}((6N+1)^2L$. Hence, the overall complexity of the proposed GASDRSE to detect 64-QAM FTN signaling will be in the order of $\mathcal{O}((6N+1)^{3.5} + (6N+1)^2L)$, which is still polynomial.

The computational complexity reduction of the proposed STSDRSE technique, when compared to the proposed GASDRSE, comes from the fact that the dimension of the unknown matrix $\mathbf{\Psi}$ is $(2N+1) \times (2N+1)$ which is smaller than its counterpart $\mathbf{\Omega}$ of $(4N+1) \times (4N+1)$ of the proposed GASDRSE. Accordingly, the computational complexity of the proposed STSDRSE technique is $\mathcal{O}((2N+1)^{3.5} + (2N+1)^2L)$.

B. SOFT-OUTPUTS

The proposed GASDRSE and STSDRSE schemes produce hard-output, and in their current forms they may not be suitable to be used with channel coding. Fortunately, Gaussian randomization can be effectively used to reduce the complexity of evaluating the log-likelihood ratio (LLR) as follows. Inspired by the idea of the list sphere decoding in [20], the Gaussian randomization step can store a list of vectors that achieve the lowest values of the objective function (instead of storing only one vector that achieves the minimum objective value). This candidate list can then be used to approximate the LLR calculations. In other words, instead of searching the whole search space, Gaussian randomization can efficiently produce candidate vectors that contribute more towards the calculation of the LLR equation. However, there is a possibility that some bit positions in the candidate list are empty. In this case, we can extend the candidate list to include all bit vectors with hamming distance of 1 of the bit vectors in the original candidate list as in [21].

VI. SIMULATION RESULTS

In this section, we evaluate the performance of the proposed GASDRSE and STSDRSE techniques in detecting 16-QAM FTN signaling. We employ an rRC filter[4] with roll-off factors $\beta = 0.3$ and 0.5. The length of the ISI is set to 23 symbols and the number of randomization iterations L is set to 1000.

A. PERFORMANCE OF THE PROPOSED GASDRSE AND STSDRSE TECHNIQUES

Fig. 2 depicts the BER of 16-QAM FTN signaling as a function of E_b/N_0 for both the proposed GASDRSE and STSDRSE techniques for $\beta = 0.3$ and $\tau = 0.7$ and 0.8. As can be seen, in general both the proposed GASDRSE

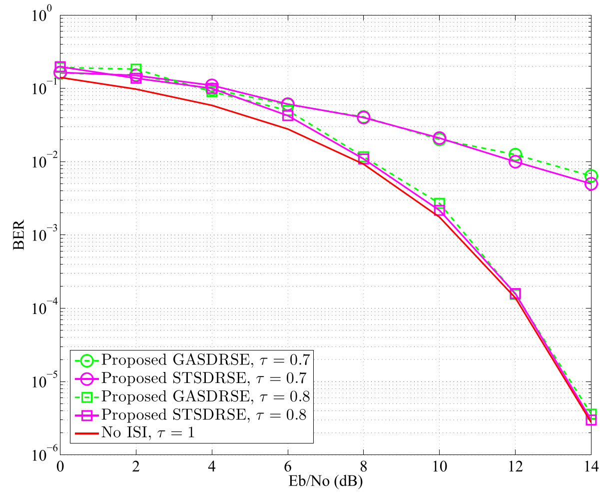

FIGURE 2. BER performance of 16-QAM FTN signaling as a function of E_b/N_0 for the proposed GASDRSE and STSDRSE techniques for $\beta = 0.3$ and $\tau = 0.7$ and 0.8.

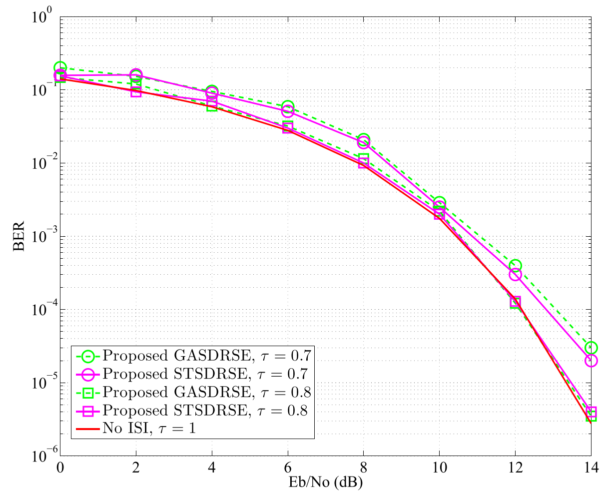

FIGURE 3. BER performance of 16-QAM FTN signaling as a function of E_b/N_0 for the proposed GASDRSE and STSDRSE techniques for $\beta = 0.5$ and $\tau = 0.7$ and 0.8.

and STSDRSE techniques almost achieve the BER performance of Nyquist signaling at $\tau = 0.8$. This means that the proposed GASDRSE and STSDRSE techniques can achieve $\frac{1}{0.8} - 1 = 25\%$ increase in the data rate, when compared to Nyquist signaling at $\beta = 0.3$, without increasing the BER, the bandwidth, or the data symbols energy. Additionally, one can notice that as the value of τ increases from 0.8 and 0.7 (i.e., the ISI between adjacent symbols increases), the BER performance deteriorates as expected. This clearly shows that our proposed algorithms provide sub-optimal solutions to the 16-QAM FTN signaling detection problem, as they cannot achieve the orthogonal error performance with τ at the Mazo limit, which for $\beta = 0.3$ lies at $\tau = 0.7$ [3].

Fig. 3 plots the BER of 16-QAM FTN signaling as a function of E_b/N_0 for both the proposed GASDRSE and STSDRSE techniques for $\beta = 0.5$ and $\tau = 0.7$ and 0.8.

[4] It is worthy to mention that the proposed GASDRSE and STSDRSE techniques are independent of the pulse shape, and they can be used with other pulse shapes, e.g., Gaussian pulses.

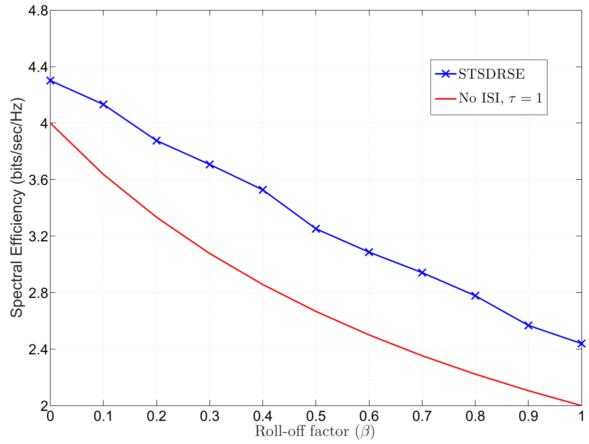

FIGURE 4. Spectral efficiency of 16-QAM FTN signaling as a function of β using the proposed STSDRSE at BER = 10^{-4}.

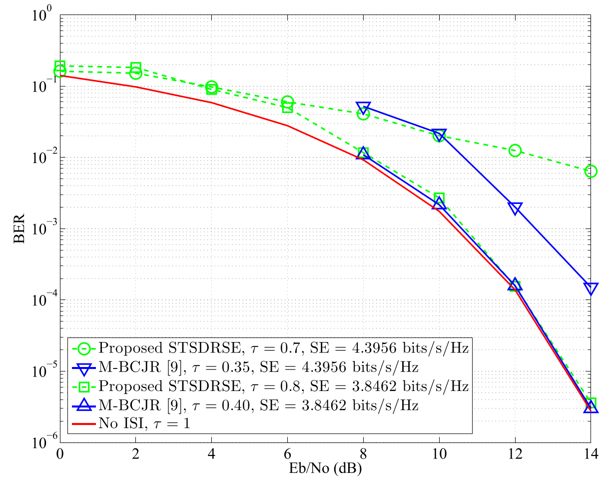

FIGURE 5. Performance comparison between 16-QAM FTN detection using the proposed STSDRSE technique and QPSK FTN signaling detection using the scheme in [9], for $\beta = 0.3$ and same spectral efficiencies of 4.3956 and 3.8462 bits/s/Hz.

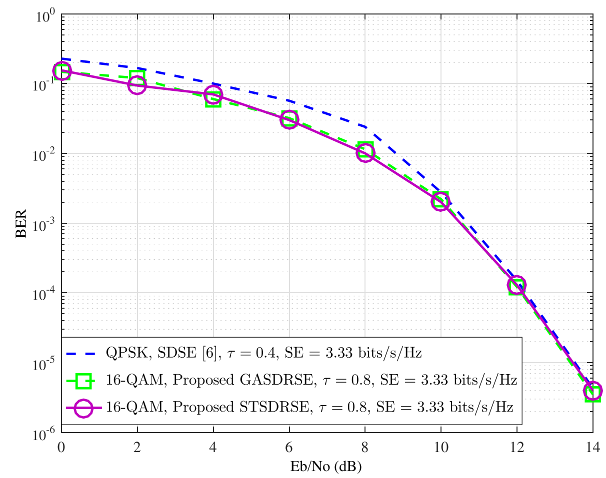

FIGURE 6. Performance comparison between 16-QAM FTN detection using the proposed GASDRSE and STSDRSE techniques and QPSK FTN signaling optimal detection using the sphere decoding in [6], for $\beta = 0.5$ and same spectral efficiency of 3.33 bits/s/Hz.

One can see from Fig. 3 that up to 24.72% increase in the data rate of 16-QAM FTN signaling can be achieved for $\tau = 0.8$ and $\beta = 0.5$, without increasing the BER, the bandwidth, or the data symbols energy, when compared to 16-QAM Nyquist signaling. Additionally, up to 42.86% increase in the data rate can be achieved for $\tau = 0.7$ and $\beta = 0.5$ at BER = 10^{-4} at the expense of 0.7 dB increase in the SNR.

Fig. 4 plots the spectral efficiency of 16-QAM Nyquist (i.e., no ISI and $\tau = 1$) and the proposed STSDRSE[5] of 16-QAM FTN signaling as a function of the roll-off factor β at the same SNR and BER = 10^{-4}. In order to have a fair comparison, the value of τ of the 16-QAM FTN signaling is selected to be the smallest value such that the proposed STSDRSE achieves the same BER = 10^{-4} of 16-QAM Nyquist signaling at the same SNR. As can be seen, the spectral efficiency of 16-QAM FTN signaling is higher than its counterpart of Nyquist signaling for all values of β. For instance, at $\beta = 0$ the proposed STSDRSE improves the spectral efficiency by 7.53% for the same BER and SNR values, when compared to Nyquist signaling. Further, the improvement of the spectral efficiency increases with increasing the value of the roll-off factor β. Additionally, results revealed that the proposed STSDRSE can achieve spectral efficiency higher than the maximum spectral efficiency of 16-QAM Nyquist signaling (4 bits/s/Hz achieved at $\beta = 0$) for the range of $\beta \in [0, 0.15]$.

B. PERFORMANCE COMPARISON WITH QUASI-OPTIMAL DETECTORS

In Fig. 5, we compare the performance of 16-QAM FTN signaling detection using the proposed STSDRSE technique and QPSK FTN signaling detection using the scheme in [9], for $\beta = 0.3$ and same spectral efficiencies of 4.3956 and 3.8462 bits/s/Hz. As can be seen, the proposed STSDRSE provides a trade-off between complexity and performance. For instance, the scheme in [9] (that operates at $\tau = 0.35$ and spectral efficiency of 4.3956 bits/s/Hz) achieves better performance than the proposed STSDESE technique (that operates at $\tau = 0.7$ and spectral efficiency of 4.3956 bits/s/Hz), at the expense of higher computational complexity. In addition, the proposed STSDRSE technique (that operates at $\tau = 0.8$ and spectral efficiency of 3.8462 bits/s/Hz) achieves the same performance as the scheme in [9] (that operates at $\tau = 0.4$ and spectral efficiency of 3.8462 bits/s/Hz), with reduced computational complexity.

Fig. 6 compares the performance of 16-QAM FTN signaling detection using the proposed GASDRSE and STSDRSE techniques and QPSK FTN signaling optimal detection using the SDSE technique in [6], for $\beta = 0.5$ and same spectral efficiency of 3.33 bits/s/Hz. Although both 16-QAM and QPSK FTN signaling have the same BER performance for

[5]Spectral efficiency results of the proposed GASDRSE are not included as it is similar to that of the STSDRSE as shown in Figs. 2 and 3.

$\beta = 0.5$ and SE of 3.33 bits/s/Hz, but as mentioned earlier the computational complexity of the proposed GASDRSE and STSDRSE is much lower than its counterpart of the SDSE technique required to detect QPSK FTN signaling.

VII. CONCLUSION

FTN signaling is a promising transmission technique to significantly improve the spectral efficiency, when compared to Nyquist signaling. In this paper, we presented the first attempt in the literature to detect any high-order QAM FTN signaling, in polynomial time complexity. More specifically, we introduced a general approach to model the finite alphabet of any high-order QAM constellation as a high degree polynomial constraint, and we formulated the high-order QAM FTN signaling detection problem as a non-convex optimization problem that turns out to be NP-hard to solve. We showed that for 16-QAM, the high degree polynomial can be replaced with multiple quadratic constraints, with the help of auxiliary variables. This enabled us to propose a GASDRSE technique that efficiently provides a sub-optimal solution to the NP-hard non-convex FTN detection problem with polynomial time complexity. For the 16-QAM FTN signaling, we additionally proposed a STSDRSE technique that is of lower complexity when compared to the GASDRSE technique. Simulation results showed that up to 25% increase in the data rate can be achieved at $\beta = 0.3$ without increasing the BER, the bandwidth, or the data symbols energy, when compared to Nyquist signaling; or up to 42.86% increase in the data rate can be achieved at $\beta = 0.5$ with 0.7 dB penalty in the SNR. Additionally, results revealed that the proposed STSDRSE can achieve spectral efficiency higher than the maximum spectral efficiency of 16-QAM Nyquist signaling (4 bit/s/Hz achieved at $\beta = 0$) for the range of $\beta \in [0, 0.15]$ for the same BER and SNR.

APPENDIX
COVARIANCE OF NOISE VECTOR η

The covariance matrix of the noise vector $\boldsymbol{\eta}$ can be calculated as

$$\begin{aligned}\mathbb{E}\{\boldsymbol{\eta}\boldsymbol{\eta}^{\mathrm{T}}\} &= \mathbb{E}\{\boldsymbol{G}^{-1}\boldsymbol{q}_{\mathrm{c}}\boldsymbol{q}_{\mathrm{c}}^{\mathrm{T}}(\boldsymbol{G}^{-1})^{\mathrm{T}}\} \\ &= \boldsymbol{G}^{-1}\mathbb{E}\{\boldsymbol{q}_{\mathrm{c}}\boldsymbol{q}_{\mathrm{c}}^{\mathrm{T}}\}(\boldsymbol{G}^{-1})^{\mathrm{T}}. \end{aligned} \tag{49}$$

Given that the real noise vector is $\boldsymbol{q}_{\mathrm{c}} = [\Re\{\overline{\boldsymbol{q}}\}^{\mathrm{T}}, \Im\{\overline{\boldsymbol{q}}\}^{\mathrm{T}}]^{\mathrm{T}}$, the value of $\mathbb{E}\{\boldsymbol{q}_{\mathrm{c}}\boldsymbol{q}_{\mathrm{c}}^{\mathrm{T}}\}$ can be calculated as

$$\mathbb{E}\{\boldsymbol{q}_{\mathrm{c}}\boldsymbol{q}_{\mathrm{c}}^{\mathrm{T}}\} = \begin{bmatrix}\mathbb{E}\{\Re\{\overline{\boldsymbol{q}}_{\mathrm{c}}\}\Re\{\overline{\boldsymbol{q}}_{\mathrm{c}}\}^{\mathrm{T}}\} & \mathbb{E}\{\Re\{\overline{\boldsymbol{q}}_{\mathrm{c}}\}\Im\{\overline{\boldsymbol{q}}_{\mathrm{c}}\}^{\mathrm{T}}\} \\ \mathbb{E}\{\Im\{\overline{\boldsymbol{q}}_{\mathrm{c}}\}\Re\{\overline{\boldsymbol{q}}_{\mathrm{c}}\}^{\mathrm{T}}\} & \mathbb{E}\{\Im\{\overline{\boldsymbol{q}}_{\mathrm{c}}\}\Im\{\overline{\boldsymbol{q}}_{\mathrm{c}}\}^{\mathrm{T}}\}\end{bmatrix}. \tag{50}$$

The values of $\mathbb{E}\{\Re\{\overline{\boldsymbol{q}}_{\mathrm{c}}\}\Re\{\overline{\boldsymbol{q}}_{\mathrm{c}}\}^{\mathrm{T}}\}$ and $\mathbb{E}\{\Re\{\overline{\boldsymbol{q}}_{\mathrm{c}}\}\Im\{\overline{\boldsymbol{q}}_{\mathrm{c}}\}^{\mathrm{T}}\}$ can be calculated with the help of $\mathbb{E}\{\overline{\boldsymbol{q}}_{\mathrm{c}}\overline{\boldsymbol{q}}_{\mathrm{c}}^{\mathrm{H}}\} = \sigma^2\overline{\boldsymbol{G}}$ as follows.

$$\begin{aligned}\mathbb{E}\{\overline{\boldsymbol{q}}_{\mathrm{c}}\overline{\boldsymbol{q}}_{\mathrm{c}}^{\mathrm{H}}\} &= \mathbb{E}\{(\Re\{\overline{\boldsymbol{q}}_{\mathrm{c}}\} + j\Im\{\overline{\boldsymbol{q}}_{\mathrm{c}}\})(\Re\{\overline{\boldsymbol{q}}_{\mathrm{c}}\}^{\mathrm{T}} - j\Im\{\overline{\boldsymbol{q}}_{\mathrm{c}}\}^{\mathrm{T}})\} \\ &= \mathbb{E}\{\Re\{\overline{\boldsymbol{q}}_{\mathrm{c}}\}\Re\{\overline{\boldsymbol{q}}_{\mathrm{c}}\}^{\mathrm{T}}\} + \mathbb{E}\{\Im\{\overline{\boldsymbol{q}}_{\mathrm{c}}\}\Im\{\overline{\boldsymbol{q}}_{\mathrm{c}}\}^{\mathrm{T}}\} \\ &\quad + j\mathbb{E}\{\Im\{\overline{\boldsymbol{q}}_{\mathrm{c}}\}\Re\{\overline{\boldsymbol{q}}_{\mathrm{c}}\}^{\mathrm{T}}\} - j\mathbb{E}\{\Re\{\overline{\boldsymbol{q}}_{\mathrm{c}}\}\Im\{\overline{\boldsymbol{q}}_{\mathrm{c}}\}^{\mathrm{T}}\}. \\ &= \sigma^2\overline{\boldsymbol{G}} \end{aligned} \tag{51}$$

We assume that $\mathbb{E}\{\Im\{\overline{\boldsymbol{q}}_{\mathrm{c}}\}\Re\{\overline{\boldsymbol{q}}_{\mathrm{c}}\}^{\mathrm{T}}\} = \mathbb{E}\{\Re\{\overline{\boldsymbol{q}}_{\mathrm{c}}\}\Im\{\overline{\boldsymbol{q}}_{\mathrm{c}}\}^{\mathrm{T}}\} = 0$ (this assumption can be further verified from the fact that $p(t)$ is real-valued, and hence, $\Im\{\overline{\boldsymbol{G}}\} = 0$ for the considered AWGN case; accordingly, $\sigma^2\overline{\boldsymbol{G}}$ does not have imaginary parts). Accordingly, (51) is re-written as

$$\mathbb{E}\{\Re\{\overline{\boldsymbol{q}}_{\mathrm{c}}\}\Re\{\overline{\boldsymbol{q}}_{\mathrm{c}}\}^{\mathrm{T}}\} + \mathbb{E}\{\Im\{\overline{\boldsymbol{q}}_{\mathrm{c}}\}\Im\{\overline{\boldsymbol{q}}_{\mathrm{c}}\}^{\mathrm{T}}\} = \sigma^2\overline{\boldsymbol{G}}. \tag{52}$$

We also assume that the noise is a proper random variable, i.e. its real and imaginary parts have equal variance [22]; that said we can conclude that

$$\mathbb{E}\{\Re\{\overline{\boldsymbol{q}}_{\mathrm{c}}\}\Re\{\overline{\boldsymbol{q}}_{\mathrm{c}}\}^{\mathrm{T}}\} = \mathbb{E}\{\Im\{\overline{\boldsymbol{q}}_{\mathrm{c}}\}\Im\{\overline{\boldsymbol{q}}_{\mathrm{c}}\}^{\mathrm{T}}\} = \frac{1}{2}\sigma^2\overline{\boldsymbol{G}}. \tag{53}$$

By substituting (53) into (50), we get

$$\begin{aligned}\mathbb{E}\{\boldsymbol{q}_{\mathrm{c}}\boldsymbol{q}_{\mathrm{c}}^{\mathrm{T}}\} &= \begin{bmatrix}\frac{1}{2}\sigma^2\overline{\boldsymbol{G}} & 0 \\ 0 & \frac{1}{2}\sigma^2\overline{\boldsymbol{G}}\end{bmatrix}, \\ &= \frac{1}{2}\sigma^2\boldsymbol{G}, \end{aligned} \tag{54}$$

which is reached by knowing that $\Re\{\overline{\boldsymbol{G}}\} = \overline{\boldsymbol{G}}$ and $\Im\{\overline{\boldsymbol{G}}\} = 0$ for the considered AWGN case. Finally, from (49) and (54), one can easily find that $\mathbb{E}\{\boldsymbol{\eta}\boldsymbol{\eta}^{\mathrm{T}}\} = \frac{1}{2}\sigma^2\boldsymbol{G}^{-1}$.

REFERENCES

[1] J. B. Anderson, F. Rusek, and V. Öwall, "Faster-than-Nyquist signaling," *Proc. IEEE*, vol. 101, no. 8, pp. 1817–1830, Aug. 2013.

[2] J. E. Mazo, "Faster-than-Nyquist signaling," *Bell Syst. Tech. J.*, vol. 54, no. 8, pp. 1451–1462, 1975.

[3] A. D. Liveris and C. N. Georghiades, "Exploiting faster-than-Nyquist signaling," *IEEE Trans. Commun.*, vol. 51, no. 9, pp. 1502–1511, Sep. 2003.

[4] F. Rusek and J. B. Anderson, "The two dimensional Mazo limit," in *Proc. Int. Symp. Inf. Theory (ISIT)*, Sep. 2005, pp. 970–974.

[5] F. Rusek, "On the existence of the Mazo-limit on MIMO channels," *IEEE Trans. Wireless Commun.*, vol. 8, no. 3, pp. 1118–1121, Mar. 2009.

[6] E. Bedeer, H. Yanikomeroglu, and M. H. Ahmed, "Reduced complexity optimal detection of binary faster-than-Nyquist signaling," in *Proc. IEEE Int. Conf. Commun. (ICC)*, Paris, France, 2017, pp. 1–6.

[7] A. Prlja, J. B. Anderson, and F. Rusek, "Receivers for faster-than-Nyquist signaling with and without turbo equalization," in *Proc. IEEE Int. Symp. Inf. Theory*, Jul. 2008, pp. 464–468.

[8] J. B. Anderson, A. Prlja, and F. Rusek, "New reduced state space BCJR algorithms for the ISI channel," in *Proc. IEEE Int. Symp. Inf. Theory (ISIT)*, Jun. 2009, pp. 889–893.

[9] J. B. Anderson and A. Prlja, "Turbo equalization and an M-BCJR algorithm for strongly narrowband intersymbol interference," in *Proc. IEEE Int. Symp. Inf. Theory Appl. (ISIT)*, Jun. 2010, pp. 261–266.

[10] E. Bedeer, M. H. Ahmed, and H. Yanikomeroglu, "A very low complexity successive symbol-by-symbol sequence estimator for faster-than-Nyquist signaling," *IEEE Access*, vol. 5, pp. 7414–7422, Mar. 2017.

[11] J. B. Anderson, "A review of faster than Nyquist signaling with an extension to four-level modulation," in *Proc. 9th Int. Symp. Turbo Codes Iterative Inf. Process. (ISTC)*, Sep. 2016, pp. 6–10.

[12] J. Zhang, J. Yu, and N. Chi, "Generation and transmission of 512-Gb/s quad-carrier digital super-Nyquist spectral shaped signal," *Opt. Exp.*, vol. 21, no. 25, pp. 31212–31217, Dec. 2013.

[13] S. Arora and B. Barak, *Computational Complexity: A Modern Approach*. Cambridge, U.K.: Cambridge Univ. Press, 2009.

[14] J. Proakis, *Digital Communications*. New York, NY, USA: McGraw-Hill, 2001.

[15] A. V. Oppenheim and R. W. Schafer, *Discrete-Time Signal Processing*. Upper Saddle River, NJ, USA: Pearson Ed., 2010.

[16] W.-K. Ma, *Semidefinite Relaxation and its Applications in Signal Processing and Communications*. Xi'an, China: MIIS Tutorial, Jul. 2012.

[17] Z.-Q. Luo, W.-K. Ma, A. M.-C. So, Y. Ye, and S. Zhang, "Semidefinite relaxation of quadratic optimization problems," *IEEE Signal Process. Mag.*, vol. 27, no. 3, pp. 20–34, May 2010.

[18] M. Grant and S. Boyd. (2010). *CVX: MATLAB Software for Disciplined Convex Programming*. [Online]. Available: https://cvxr.com/cvx

[19] K. H. Rosen and K. Krithivasan, *Discrete Mathematics and Its Applications*. New York, NY, USA: McGraw-Hill, 1995.

[20] B. M. Hochwald and S. ten Brink, "Achieving near-capacity on a multiple-antenna channel," *IEEE Trans. Commun.*, vol. 51, no. 3, pp. 389–399, Mar. 2003.

[21] D. J. Love, S. Hosur, A. Batra, and R. W. Heath, "Space-time chase decoding," *IEEE Trans. Wireless Commun.*, vol. 4, no. 5, pp. 2035–2039, Sep. 2005.

[22] F. D. Neeser and J. L. Massey, "Proper complex random processes with applications to information theory," *IEEE Trans. Inf. Theory*, vol. 39, no. 4, pp. 1293–1302, Jul. 1993.

EBRAHIM BEDEER (S'10–M'14) received the B.Sc. (Hons.) and M.Sc. degrees from Tanta University, Tanta, Egypt, and the Ph.D. degree from the Memorial University of Newfoundland, St. Johns, NL, Canada, all in Electrical Engineering. He was a Post-Doctoral Fellow with The University of British Columbia, BC, Canada. He is currently a Post-Doctoral Fellow with Carleton University, Ottawa, ON, Canada. His current research interests include wireless communications and signal processing, with a current focus of resource management in wireless networks, and applications of optimization is signal processing.

Dr. Bedeer is an Editor of the IEEE Communications Letters. He has served on the Technical Program Committees of numerous major international communication conferences, such as the IEEE GLOBECOM, the IEEE ICC, the IEEE VTC, and CROWNCOM. He received numerous awards, including the Exemplary Reviewer of the IEEE Communications Letters and the IEEE Wireless Communications Letters.

MOHAMED HOSSAM AHMED (SM'07) received the Ph.D. degree in electrical engineering from Carleton University, Ottawa, in 2001. From 2001 to 2003, he was with Carleton University as a Senior Research Associate. In 2003, he joined the Faculty of Engineering and Applied Science, Memorial University of Newfoundland, where he is currently a Full Professor. He has authored over 135 papers in international journals and conferences. His research interests include radio resource management in wireless networks, multi-hop relaying, cooperative communication, vehicular ad-hoc networks, cognitive radio networks, and wireless sensor networks. His research is sponsored by NSERC, CFI, QNRF, Bell/Aliant, and other governmental and industrial agencies. He received the Ontario Graduate Scholarship for Science and Technology in 1997, the Ontario Graduate Scholarship in 1998, 1999, and 2000, and the Communication and Information Technology Ontario Graduate Award in 2000. He served as a Co-Chair of the Signal Processing Track in ISSPIT'14, the Transmission Technologies Track in VTC'10-Fall, and the Multimedia And Signal Processing Symposium in CCECE'09. He serves as an Editor of the IEEE Communication Surveys and Tutorials and as an Associate Editor of the *Wiley International Journal of Communication Systems* and the *Wiley Communication and Mobile Computing*. He served as a Guest Editor of a special issue on Fairness of Radio Resource Allocation, the *PEURASIP JWCN* in 2009, and a special issue on Radio Resource Management in Wireless Internet, the *Wiley Wireless and Mobile Computing Journal* in 2003. He is a registered Professional Engineer in the province of Newfoundland, Canada.

HALIM YANIKOMEROGLU (F'17) was born in Giresun, Turkey, in 1968. He received the B.Sc. degree in electrical and electronics engineering from the Middle East Technical University, Ankara, Turkey, in 1990, and the M.A.Sc. degree in electrical engineering and the Ph.D. degree in electrical and computer engineering from the University of Toronto, Canada, in 1992 and 1998, respectively.

During 1993–1994, he was with the Research and Development Group, Marconi Kominikasyon A.S., Ankara. Since 1998, he has been with the Department of Systems and Computer Engineering, Carleton University, Ottawa, Canada, where he is currently a Full Professor. His research interests include wireless technologies with a special emphasis on cellular networks. In recent years, his research has been funded by Huawei, Telus, Allen Vanguard, Blackberry, Samsung, Communications Research Center of Canada, and DragonWave. This collaborative research resulted in about 25 patents.

Dr. Yanikomeroglu is a Distinguished Lecturer of the IEEE Communications Society and a Distinguished Speaker for the IEEE Vehicular Technology Society in 5G wireless technologies. He has been involved in the organization of the IEEE Wireless Communications and Networking Conference (WCNC) from its inception in 1998 in various capacities, including serving as a Steering Committee Member, Executive Committee Member, and the Technical Program Chair or Co-Chair of WCNC, Atlanta, in 2004, WCNC, Las Vegas, in 2008, and WCNC, Istanbul, in 2014. He was the General Co-Chair of the IEEE 72nd Vehicular Technology Conference (VTC2010-Fall) held in Ottawa. He is currently the General Co-Chair of the IEEE 86th Vehicular Technology Conference (VTC2017-Fall) to be held in Toronto. He was the Chair of the Wireless Technical Committee. He has served in the Editorial Board of the IEEE Transactions on Communications, the IEEE Transactions on Wireless Communications, and the IEEE Communications Surveys and Tutorials.

He spent the 2011–2012 academic year with the TOBB University of Economics and Technology, Ankara, as a Visiting Professor. He is a registered Professional Engineer in the province of Ontario, Canada. He was a recipient of the IEEE Ottawa Section Outstanding Educator Award in 2014, the Carleton University Faculty Graduate Mentoring Award in 2010, the Carleton University Graduate Students Association Excellence Award in Graduate Teaching in 2010, and the Carleton University Research Achievement Award in 2009.